

Generative Latent Neural PDE Solver using Flow Matching

Zijie Li[†], Anthony Zhou[†], Amir Barati Farimani^{†*}

[†] *Department of Mechanical Engineering, Carnegie Mellon University*

Abstract

Autoregressive next-step prediction models have become the *de-facto* standard for building data-driven neural solvers to forecast time-dependent partial differential equations (PDEs). Denoise training that is closely related to diffusion probabilistic model has been shown to enhance the temporal stability of neural solvers, while its stochastic inference mechanism enables ensemble predictions and uncertainty quantification. In principle, such training involves sampling a series of discretized diffusion timesteps during both training and inference, inevitably increasing computational overhead. In addition, most diffusion models apply isotropic Gaussian noise on structured, uniform grids, limiting their adaptability to irregular domains. We propose a latent diffusion model for PDE simulation that embeds the PDE state in a lower-dimensional latent space, which significantly reduces computational costs. Our framework uses an autoencoder to map different types of meshes onto a unified structured latent grid, capturing complex geometries. By analyzing common diffusion paths, we propose to use a coarsely sampled noise schedule from flow matching for both training and testing. Numerical experiments show that the proposed model outperforms several deterministic baselines in both accuracy and long-term stability, highlighting the potential of diffusion-based approaches for robust data-driven PDE learning.

1 Introduction

Data-driven neural solvers have emerged as promising surrogates for simulating partial differential equations (PDEs), offering remarkable speed-ups over traditional numerical methods. Despite their attractive properties, recent studies [1–4] reveal that purely neural solutions often struggle with temporal stability, particularly in chaotic, time-dependent systems. Compounding errors frequently arise from the distribution shift between training and inference. The distribution shift primarily stems from the spectral bias of neural network prediction [5], which causes inaccuracies in the modeling of high-frequency components. Although such errors might not be pronounced in the single-step prediction, they gradually propagate across the entire frequency spectrum over the course of the simulation.

A straightforward way to mitigate this problem is training perturbation, in which the model input is deliberately perturbed during training to emulate the distribution shift observed in inference. A common choice for perturbation is isotropic Gaussian noise [6, 7], where the specific noise level typically depends on the problem at hand and requires tuning. Backpropagation Through Time (BPTT) [8] is a promising alternative that has been shown to effectively improve the stability of neural solvers across a variety of physical systems [1, 4, 9]. By unrolling the neural surrogate over multiple timesteps during training, it offers two practical advantages: (1) the model can see its own prediction which reduces the gap between training data and testing data, and (2) it is optimized on a multi-step loss that promotes long-term stability. Despite its effectiveness, BPTT substantially raises training costs by requiring model simulations and storing intermediate activations over the unrolled trajectory. In addition, extending backpropagation over many timesteps can lead to unstable gradients, complicating the optimization. Truncating the backpropagation chain, for example, using the pushforward technique proposed in Brandstetter *et al.* [1], can reduce computational demands. Nevertheless, because simulation is still required during training, its overall cost remains higher than that of the standard next-step regression.

Recently, the success of diffusion probabilistic models [10–12] in image generation has sparked a rapid expansion of their application to PDE-related problems [3, 13–19]. The denoising training target and multi-step sampling are found to alleviate the spectral bias of neural network prediction, which is particularly

*Correspondence: barati@cmu.edu

important for achieving stable long-term prediction in PDE simulation. In particular, the training of diffusion models are simulation-free, which are much more efficient than BPTT. The probabilistic nature of diffusion models also opens up a new venue for approaching the simulation of highly chaotic systems like 3D turbulence [20]. Achieving accurate long-term prediction on turbulent systems often requires resolving small-scale physics that demands very fine spatio-temporal discretization, and even a very minor error made in early prediction can result in significantly different future states. Instead of reproducing the exact individual trajectory, diffusion models can generate diverse possible states that remain statistically consistent.

Although diffusion models show promise for predicting and simulating time-dependent PDEs, they also pose notable challenges. In particular, their multi-step characteristic significantly raises computational costs during inference. Moreover, training these models can be computationally intensive due to slow convergence [21]: they rely on Monte Carlo sampling of diffusion time steps to approximate the integral in the evidence lower bound [11] or the denoise score matching objective [12, 22]. In this work, we propose to address these challenges from two complementary perspectives. First, we analyze different diffusion paths commonly used in generative image modeling, including the Denoising Diffusion Probabilistic Model (DDPM) [11] and more recent flow matching approaches [23, 24], and we find that a coarsely truncated noise schedule empirically works well. This reduces the number of diffusion training steps needed for both training and sampling. Second, we propose to do diffusion in a unified mesh-reduced latent space, leveraging an autoencoder that is designed to map functions sampled on disparate, irregular meshes into a structured compressed latent space. This dimensionality reduction enables a streamlined pipeline for training and deploying diffusion-based neural PDE solvers more efficiently. In addition, by trading off a certain degree of local (per-frame) accuracy, we achieve more stable predictions in the mesh-reduced space, a concept somewhat analogous to pseudo-spectral methods, where high-frequency modes are filtered to balance global stability and local accuracy.

2 Related Works

Neural PDE solver Neural networks can learn and approximate solution mappings in PDE problems directly from data [25–27], utilizing mesh-specific architectures such as convolutional layers for uniform grids [7, 28, 29] or graph-based layers for unstructured meshes [1, 6, 30–33]. Neural operators [34, 35] aim to learn a continuous mapping between input and target functions for a family of PDEs, potentially allowing them to use a single set of parameters across varying discretizations. The practical realization of it includes the learned transformation in different spectral spaces [36–38], non-linear kernel parameterized with message passing graph neural network [39, 40] or kernel parameterized with dot-product attention [41–45]. In addition, neural network can also be used to parameterize the solution function of a single instance of PDE and optimized in a data-free manner, which is known as Physics-Informed Neural Networks (PINNs) [46]. The physics-informed loss can also be applied data-driven neural operator to improve accuracy and generalization [47, 48].

Neural solver on reduced-order representations Reduced Order Modeling (ROM) [49] is widely employed to build low-dimensional, computationally efficient representations of high-dimensional dynamical systems. The reduced latent vector can be obtained from data through linear projection, e.g. proper orthogonal decomposition [50], non-linear projection methods like neural-network-based autoencoder [51–54] or learned basis function [55–57]. The temporal dynamics can be linearized and modeled with Koopman operator [58, 59], or directly modeled with neural networks [60–65]. Reducing the dimensionality of the discretized vector significantly lowers the training cost of a neural network operating in the reduced space, which enables longer BPTT horizon for more stable dynamics forecasting [66, 67].

Temporal stability of neural solver For numerical solvers that employ an explicit scheme, Courant-Friedrichs-Lewy (CFL) condition poses a constraint on temporal discretization for controlling the propagation of local approximation error. For neural solvers, they are not restricted from such constraints but the propagation of the local error are often unbounded. Common remedies include training perturbation (e.g. noise injection) [6], BPTT with unrolled training [4, 9, 66] and truncated BPTT [1]. Empirical evidence indicates that aliasing-related spectrum artifacts substantially contribute to rollout instability in certain neural network architectures [68–70]. Techniques like low-pass filtering have been shown to suppress these artifacts and improve stability. Neural solvers can also be improved through physics-guided post-processing.

For instance, Li *et al.* [2] shows that enforcing dissipativity on the network’s predictions enhances long-term statistical accuracy. Cao *et al.* [71] proposes a spectral fine-tuning method for fine-tuning neural solver with functional-type norm to minimize the residual that reaches accuracy comparable to numerical solvers on temporal forecasting of 2D fluid flow while being highly efficient.

Diffusion probabilistic models in PDEs The success of diffusion models in image generation [11, 72] has spurred growing interest in applying diffusion model for PDE problems. Shu *et al.* [14] proposes to incorporate the constraint of the solution manifold [73], i.e. the residual information of the PDEs, into the posterior sampling process for solving inverse problem in fluid field reconstruction. Lippe *et al.* [3] find that denoising training target can effectively alleviate spectral bias in neural network prediction and propose a modified noise schedule for denoising training/sampling. Similar observation is made in autoregressive conditional diffusion model [15]. The conditional diffusion framework has also been applied in global weather forecasting [18], not only it improves the stability and accuracy of the forecast, but also provides uncertainty quantification of extreme event. Diffusion model can also be used for data assimilation [16, 74], uncertainty quantification [75, 76] and learning statistically coherent distribution [17, 20, 77] in PDE problems.

3 Methodology

3.1 Diffusion probabilistic model

Diffusion probabilistic models (DPMs) [10–12] are a class of generative models that reverse noise-corruption processes. Given data point $\mathbf{x}_0 \in \mathbb{R}^d$ and its associated distribution $\mathbf{x}_0 \sim p(\mathbf{x}_0)$, (Gaussian-) diffusion model defines a forward process that gradually adds Gaussian noise to the state variable \mathbf{x}_t which results in following time-dependent marginal: $q(\mathbf{x}_t|\mathbf{x}_0) = q(\mathbf{x}_t|\alpha_t\mathbf{x}_0, \sigma_t^2\mathbf{I})$, where $\alpha_t, \sigma_t \in \mathbb{R}_+$ are hyperparameters of the noising process, and are usually referred to as noising schedule. The noise schedule is chosen such that the endpoint $q(\mathbf{x}_T|\mathbf{x}_0) \approx \mathcal{N}(0, \bar{\sigma}^2\mathbf{I})$.

It has been shown that the following stochastic differential equation (SDE) result in the above transition distribution $q(\mathbf{x}_t|\mathbf{x}_0)$ [12]:

$$d\mathbf{x}_t = f(t)dt + g(t)d\mathbf{w}_t, \tag{1}$$

where $\mathbf{w}_t \in \mathbb{R}^d$ is the standard Wiener process, and

$$f(t) = \frac{d \log \alpha_t}{dt}, g^2(t) = \frac{d\sigma_t^2}{dt} - 2 \frac{d \log \alpha_t}{dt} \sigma_t^2. \tag{2}$$

Song *et al.* [12] also show that the SDE in (1) can be reversed by solving the following SDE backward in time:

$$d\mathbf{x}_t = [f(t)\mathbf{x}_t - g^2(t)\nabla_x \log q_t(\mathbf{x}_t)]dt + g(t)d\bar{\mathbf{w}}_t, \tag{3}$$

where $\bar{\mathbf{w}}_t$ is the standard Wiener process flowing reverse in time. Furthermore, there also exists an ordinary differential equation (ODE) which shares the same marginal probabilities along the trajectory $\{q_t(\mathbf{x}_t)\}$:

$$d\mathbf{x}_t = [f(t) - \frac{1}{2}g^2(t)\nabla_x \log q_t(\mathbf{x}_t)]dt. \tag{4}$$

The score function $\nabla_x \log q_t(\mathbf{x}_t)$ can be estimated with a neural network model s_θ that is trained via denoising score matching [12, 22, 78]. To generate samples, one can first sample $\mathbf{x}_T \sim \mathcal{N}(0, \bar{\sigma}^2\mathbf{I})$ and then numerically solve (3) or (4) backward in time. The ODE formulation is generally more tolerant to larger step size and thus it is widely adopted for faster sampling [79–81].

The conditional information \mathbf{y} can be plugged into the model directly to estimate the conditional score function $\nabla_x \log q_t(\mathbf{x}_t|\mathbf{y})$.

For forward problems in time-dependent PDEs, we are interested in estimating \mathbf{u}^{m+1} given: $\mathbf{u}^m, \mathbf{u}^{m-1}, \dots, \mathbf{u}^{m-h+1}, \xi$, where \mathbf{u}^m denotes the system state \mathbf{u} (e.g. velocity, pressure) at physical timestep t_m , and ξ denotes system parameters such as viscosities. The most straightforward way to achieve this would be training a regression model to predict \mathbf{u}^{m+1} . However, it is empirically observed that the long-term rollout stability for this kind of model is usually brittle despite good next-step prediction accuracy [1]. The major reason for this is the input distribution shift due to the accumulated error of the model. The discrepancy between model’s next-step prediction and ground truth in the high-frequency regime will gradually transport to the whole spectrum through the non-linear terms in the equations (e.g. $u\nabla u$), even though the error

in this regime might not be pronounced in loss function like MSE. PDE-Refiner [3] shows that recasting next-step predictor as an interpolator between noise and next-step prediction can mitigate the spectral bias of neural network’s prediction [5] and therefore improve the long-term stability. ACDM (autoregressive conditional diffusion model) [15] reformulates deterministic next-step prediction as probabilistic generation of the future state, and observes a similar trend as PDE-refiner. Despite these models are built from different perspectives but they are actually equivalent under the following viewpoint, where they are just different parameterizations of an interpolant between noise $\mathbf{x}_1 = \bar{\epsilon} \sim \mathcal{N}(0, \mathbf{I})$ and next-step state $\mathbf{x}_0 = \mathbf{u}^{m+1}$. A commonly used sampler/numerical solver for the diffusion model is DDIM [79], with the following update rule:

$$\mathbf{x}_s = \frac{\alpha_s}{\alpha_k} \mathbf{x}_k - \alpha_s \left[\frac{\sigma_k}{\alpha_k} - \frac{\sigma_s}{\alpha_s} \right] \hat{\epsilon}_k, \quad (5)$$

where $0 < s < k$, $\hat{\epsilon}$ denotes the noise prediction of the neural network. Under change of variable, $\lambda_i = \sigma_i/\alpha_i$, $\tilde{\mathbf{x}}_i = \mathbf{x}_i/\alpha_i$:

$$\tilde{\mathbf{x}}_s = \tilde{\mathbf{x}}_k - (\lambda_k - \lambda_s) \hat{\epsilon}_k. \quad (6)$$

For the SDE formulation (as the ancestral sampler in DDPM [11] and PDE-Refiner [3]) amounts to the Euler scheme in equation (6) with additional noise injection at every update:

$$\tilde{\mathbf{x}}_s = \tilde{\mathbf{x}}_k - 2(\lambda_k - \lambda_s) \hat{\epsilon}_k + \sqrt{\lambda_k^2 - \lambda_s^2} \mathbf{n}_k, \quad (7)$$

where $\mathbf{n}_k \sim \mathcal{N}(0, \mathbf{I})$. Given that $\lambda(i) = \sigma(i)/\alpha(i)$ is monotonic, (6) is the first-order Euler discretization of the following ODE:

$$d\tilde{\mathbf{x}}_\lambda = -\epsilon(\tilde{\mathbf{x}}_\lambda, \lambda) d\lambda. \quad (8)$$

Under the context of next-step prediction in temporal PDEs, if we use diffusion integration scheme to solve for the next step, considering the DDIM update in (6), the final prediction is a linear combination of a series of prediction:

$$\begin{aligned} \tilde{\mathbf{x}}_{\lambda_0} &= \tilde{\mathbf{x}}_{\lambda_1} - \hat{\epsilon}_{\lambda_1} (\lambda_1 - \lambda_0) \\ &= (\tilde{\mathbf{x}}_{\lambda_2} - \hat{\epsilon}_{\lambda_2} (\lambda_2 - \lambda_1)) - \hat{\epsilon}_{\lambda_1} (\lambda_1 - \lambda_0) \\ &= \tilde{\mathbf{x}}_{\lambda_K} - \sum_{i=1}^K \hat{\epsilon}_{\lambda_i} (\lambda_i - \lambda_{i-1}), \end{aligned} \quad (9)$$

where the diffusion temporal discretization $\{\lambda_i\}_{i=0}^K$ determines the coefficients for each neural network prediction. Interestingly, this is in the same functional form as many linear multi-step methods, such as Adams–Bashforth method. The "diffusion multi-step" method here offers several intriguing properties when building a neural PDE solver. First, it can be viewed as predictor-corrector scheme that allows the prediction error made at earlier diffusion steps being adjusted at later diffusion steps. From (9), the final weight of model can be dynamically adjusted with noise schedule α_i, σ_i . Second is that training model different levels of noise facilitates the optimization of model’s prediction at different regimes of the spectrum. Furthermore, the diffusion-based prediction effectively introduces stochasticity to the model. It is extremely difficult to obtain accurate long-term forecast for a lot of the chaotic systems that are sensitive to small perturbations. In such case, deterministic forecasting models will produce either blurry prediction or only be able to generate a single set of system state, whereas stochastic models can provide a better coverage of different modes in the distribution of possible system states.

The noise schedule is a critical factor that controls both the training and inference dynamics. ACDM [15] have explored using DDPM’s scheduler [11], which works well on image generation tasks, to temporal PDE forecasting. It is observed that the backward diffusion sampling converges within fewer DDIM steps than natural image generation. This is not surprising as for a well-determined forward problem, the distribution $p(\mathbf{u}^{m+1}|\mathbf{u}^m)$ is a Dirac delta function centered around the unique solution of \mathbf{u}^{m+1} . In contrast, conditional image generation is a many-to-one mapping problem (i.e. multiple text description can correspond to the same image and vice versa), such that too few sampling steps will result in sampling the mean of multiple possible images that is usually blurry. Therefore, forward problems in PDEs might not require much of the inference steps, and even training steps. To this end, PDE-Refiner [3] proposes a customized exponential scheduler and shows that it outperforms the DDPM scheduler. However, it requires heuristically picking a minimum noise level for the noise schedules and additionally, $\lambda_i = \alpha_i/\sigma_i$ are more shifted towards high

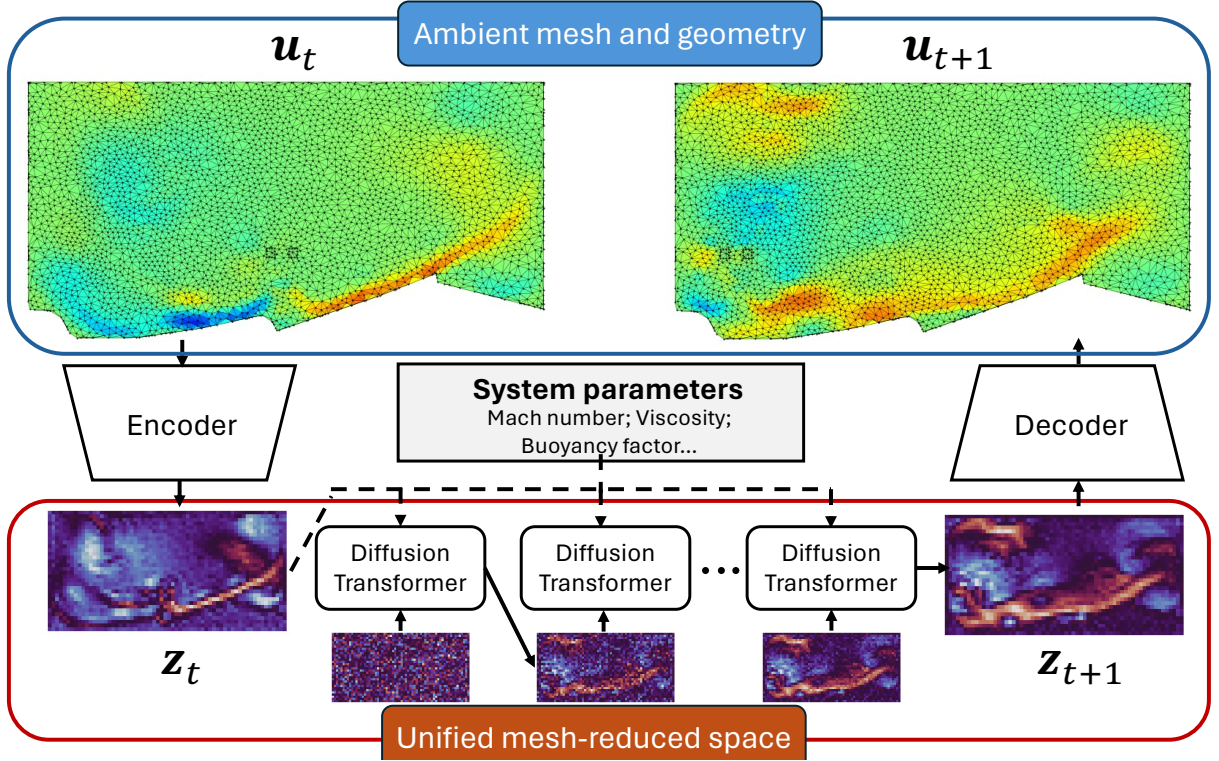


Figure 1: Main architecture of the proposed latent neural solver based on flow matching. The input data is projected onto a unified latent space via encoder. In the latent space, the diffusion model iteratively transform the noise into the latent state of future timestep. The latent embedding can be projected back to the original mesh space via the decoder.

signal-to-noise regime which might cause the input samples not perturbed enough. In this work, we propose to develop our generative latent neural PDE solver based on flow matching framework. Flow matching [23, 24] with optimal transport path and Gaussian endpoint $q_1(\mathbf{x}_1) \sim \mathcal{N}(0, \mathbf{I})$, can also be viewed as a special case of Gaussian diffusion with following noise schedule:

$$\mathbf{x}_t = (1-t)\mathbf{x}_0 + t\epsilon, \quad \epsilon \sim \mathcal{N}(0, \mathbf{I}). \quad (10)$$

Based on the above noise schedule, Lipman *et al.* [23] and Liu *et al.* [24] propose the following flow ODE: $d\mathbf{x}_t = -\mathbf{v}(\mathbf{x}_t, t)dt$, where a neural network \mathbf{v}_θ is trained to estimate the velocity field via optimizing the conditional flow matching loss [23]. From (8), we can see that the flow matching with the optimal path shares a similar flow ODE as the standard diffusion probabilistic model up to a change of variable. Compared to the commonly used noise prediction parameterization, the velocity field prediction in flow matching target offers several practical benefits. As it avoids the irregularity at the boundary $t = 1$ during sampling that arises due to the α_1 in the denominator [82]. Additionally, flow matching’s noise schedule provides better coverage of low signal-to-noise ratio regime compared to the exponential schedule in PDE-Refiner, where we observe that it empirically performs better on mesh-reduced space.

3.2 Diffusion in a unified mesh-reduced space

The multi-step inference scheme in diffusion models, while offering certain advantages in terms of accuracy and stability, makes them more computationally expensive than a standard next-step prediction model. Moreover, as many PDE data are often represented on irregular meshes with complex geometries, which can make the Gaussian diffusion formulation less effective. Inspired by the success of latent diffusion model in image modeling [72], we propose to learn diffusion model in a latent space that features a resolution-reduced discretized field and uniform grid structure.

Autoencoder The encoder is used to project the function sampled on input meshes to latent embedding that lies on a coarsened grid, and the decoder is used to reconstruct the target function values on a set of query points. To approximate the mapping between functions and transform the discretization structure of the field (more specifically, from an irregular mesh to a uniform mesh), we leverage the learnable kernel integral proposed in Kovachki *et al.* [35], which serves as a well-suited foundational component. Specifically, we parameterize the kernel as a distance-based function and use locally truncated Monte-Carlo sampling to compute the integral numerically as in Geometry-Informed Neural Operator (GINO) [39]:

$$f(y_i) = \int_{B_r(y_i)} \kappa(y_i, y) u(y) dy \approx \sum_{j \in B_r(i)} \kappa(y_i, y_j) u(y_j) \mu_j, \quad (11)$$

where f is the output function and u is the input function, B_r denotes a local ball with radius r , μ_j is the Riemann sum weight for j -th point. (11) only requires point-based sampling, thus it is mesh-agnostic and enables altering the discretization within the model. The truncated domain reduces the number of points that need to be taken into consideration when evaluating the integral, which greatly improves model’s efficiency on high-dimensional problems. After deriving functions sampled on uniform latent grid, we use convolutional layers to further compress/reconstruct it. Despite convolutional layers are less flexible in terms of handling different grid resolutions, it is observed that they performs well on certain fixed-resolution problems [13, 83], primarily due to that the numerical accuracy of evaluating an integral on coarse mesh can be limited.

The optimization target of the autoencoder is to achieve least lossy compression of the PDE data. In the meantime, since our ultimate goal is to develop an accurate and stable temporal PDE prediction model, we want to avoid a high variance and temporal oscillating latent space. To this end, the training target for the autoencoder comprises three components - an \mathcal{L}^2 reconstruction loss, a KL divergence regularization term [84] that pushes the latent distribution towards a Gaussian prior, and temporal jerk regularization [85] that promotes the smoothness of latent dynamics.

Diffusion Transformer We parameterize the velocity predictor (of the diffusion process) using an attention-based [86] neural network architecture called Diffusion Transformer. Diffusion Transformer (DiT) performs well in the diffusion modeling of text [87] and image [88]. Given the context of previous frames’ latent encoding $\{\mathbf{z}^m, \mathbf{z}^{m-1}, \dots, \mathbf{z}^{m-h+1}\}$, system parameters ξ , a scalar indicator of the signal-to-noise ratio (here we use diffusion timestep k) and the state of prediction target at current diffusion timestep \mathbf{x}_k , the model \mathbf{v}_θ predicts the conditional velocity field \mathbf{v} of the flow ODE: $\mathbf{v}(\mathbf{x}_k, k, \mathbf{c}) = \epsilon - \mathbf{x}_0$, where $\mathbf{x}_0 = \mathbf{z}^{m+1}$, $\mathbf{x}_1 = \epsilon \sim \mathcal{N}(0, \mathbf{I})$ and \mathbf{c} contains the conditioning information of previous frames and system parameters. The loss function is defined as:

$$L_{\text{FM}} = \mathbb{E}_{k \sim p(k), \epsilon \sim \mathcal{N}(0, \mathbf{I})} \|\mathbf{v}_\theta(\mathbf{x}_k, k, \mathbf{c}) - (\epsilon - \mathbf{x}_0)\|_2^2. \quad (12)$$

To reduce the computational cost associated with data on multi-dimensional domain, we propose to replace part of the full-rank standard attention layers in DiT with multi-dimensional factorized attention proposed in Li *et al.* [43], which we find not only improves efficiency but also the accuracy on the problems we studied.

4 Experiments and Discussion

4.1 Problems

We test out the proposed model on three different time-dependent PDE problems.

2D buoyancy-driven flow This problem depicts smoke volume rising in a closed domain. The governing equations are incompressible Navier-Stokes equation coupled with advection equation. The boundary condition for the smoke field is Dirichlet and the boundary condition for the flow field is Neumann. We use the pre-generated dataset from Gupta & Brandstetter [83] that is implemented in *phiflow*[89]. The dataset contains 2496 training trajectories with varying initial conditions and buoyancy factors. The objective is to predict the scalar density field of smoke d and velocity of flow \mathbf{u} .

Magnetohydrodynamics compressible turbulence Magnetohydrodynamics (MHD) describes the behavior of electrically conducting fluids in the presence of magnetic fields and is fundamental to understanding astrophysical phenomena such as the solar wind, galaxy formation, and interstellar medium (ISM) turbulence [90]. We use the publicly available dataset from the Well [91]. This dataset consists of isothermal MHD simulations in the compressible regime. The simulations, originally generated at a resolution of 256^3 , have been downsampled to 64^3 using an ideal low-pass filter to remove aliasing artifacts. The dataset contains trajectories with different sonic Mach numbers and Alfvénic Mach numbers. The objective is to predict the density field ρ , magnetic field \mathbf{B} and velocity field \mathbf{u} .

Airflow around Unmanned Aerial Vehicle For this problem we use the EAGLE dataset [92]. The EAGLE dataset simulates airflow dynamics around a 2D Unmanned Aerial Vehicle (UAV) hovering over different floor profiles. The UAV follows a fixed trajectory while its propellers create complex turbulence interacting with the scene. Floor profiles are generated using three interpolation methods: Step (sharp angles, abrupt flow changes), Triangular (small vortices), and Spline (smooth trails, complex vortices). The dataset includes 600 geometries and 1,200 simulation trajectories. Velocity and pressure fields are simulated on a dynamically evolving triangle mesh using ANSYS Fluent, solving Reynolds-Averaged Navier-Stokes equations with a Reynolds stress turbulence model. The target is to predict the pressure field \mathbf{p} and velocity field \mathbf{u} .

4.2 Discussion

Variables	\mathbf{u}	d
FNO [36]	0.5672	0.1308
UNet [83, 93]	0.4143	0.1059
LDM (sequence) [13]	0.5384	0.2022
Latent-AR	0.4229	0.1076
Latent-FM (ens=1)	0.3786	0.0995
Latent-FM (ens=8)	0.3759	0.0992

Table 1: NRMSE of different models on buoyancy-driven flow. *ens* denotes the size of ensemble.

Variable	\mathbf{u}	d
Exponential ($\sigma_{\min}=1e-1$)	0.4837	0.1324
Exponential ($\sigma_{\min}=1e-2$)	0.4289	0.1147
Exponential ($\sigma_{\min}=1e-3$)	0.4023	0.1031
Exponential ($\sigma_{\min}=1e-6$)	0.3995	0.1005
FM (5 steps)	0.3859	0.1003
FM (10 steps)	0.3786	0.0995
FM (1000 steps *)	0.4514	0.1163

Table 2: NRMSE of different diffusion paths on buoyancy-driven flow. *: 1000 steps are used for training and 50 steps are used for sampling.

On the buoyancy-driven flow problem, we consider benchmarking against FNO, modern UNet from Gupta & Brandstetter [83], and sequence-wise latent diffusion model [13]. We also implement a deterministic predictor which also operates in the latent space derived from autoencoder. The result is listed in Table 1, which shows that the proposed flow matching predictor outperforms other deterministic baselines. The ensemble mean has slightly better accuracy over a single sampler. To study the influence of different noise schedules, we compare the performance of the model with different diffusion paths and training settings. For the exponential schedule proposed in PDE-Refiner, we alter the magnitude of σ_{\min} and compare their performance. All the exponential noise schedule based models use a sampling and training steps of 10. As for all flow matching (FM) based models, except for the 1000 steps variant, the training/sampling steps are indicated by the number in the bracket. As shown in Table 2, flow matching outperforms the exponential schedule while eliminating the need to pre-define a minimum noise level. In addition, we observe that the discretization of diffusion timesteps during training can also be truncated, as a finer discretization of the diffusion time does not bring in performance improvement.

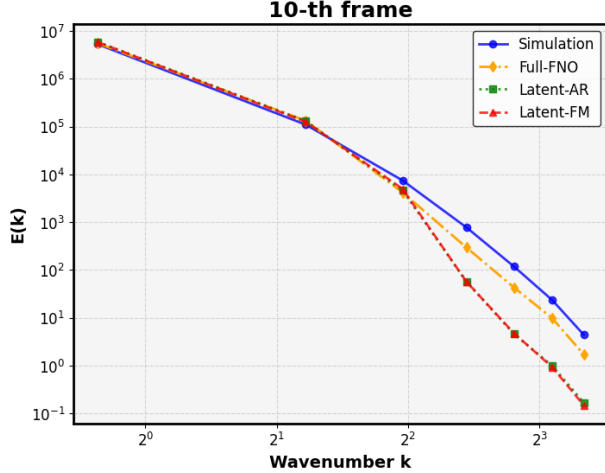


Figure 2: Spectrum averaged across a time-window centered at 10-th frame.

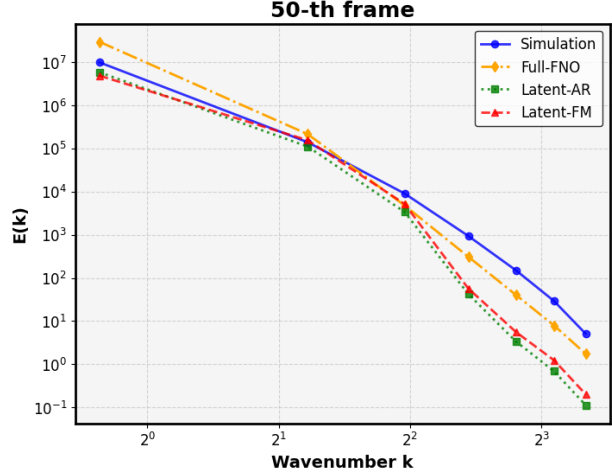


Figure 3: Spectrum averaged across a time-window centered at 50-th frame.

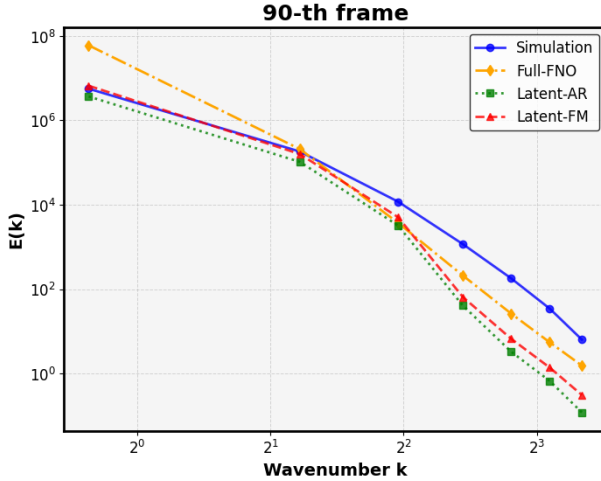


Figure 4: Spectrum averaged across a time-window centered at 90-th frame.

Time horizon	6:12	13:30
FNO	1.24	1.61
TFNO [94]	1.25	1.81
UNet	1.65	4.66
CNextUNet [91]	1.30	2.23
Latent-AR	0.89	1.25
Latent-FM (ens=1)	0.88	1.24
Latent-FM (ens=8)	0.87	1.24

Table 3: NRMSE for different model’s prediction on MHD under different rollout length.

For the 3D compressible MHD problem, we compare against the benchmark reported in the Well [91], which comprises FNO, Tensorized-FNO (TFNO) [94], UNet and a modified version of UNet using ConvNext block [95]. Compared to 2D problems, 3D turbulence exhibit more complex energy cascade due to vortex stretching. The models will need to resolve the spatiotemporal features of all scales to accurately predict the characteristics of the field. As shown in Table 3, all the models’ predictions quickly de-correlate with the reference numerical simulation after a short time period. Similar patterns have been observed in Lienen *et al.* [20], where it is infeasible for autoregressive neural solver to produce accurate long-term forecast on the chaotic 3D turbulence. Nonetheless, we are still interested at studying the behavior of model in terms of the system states it generated. To this end, we compare the spectrum of prediction generated by FNO that operates on the full-order space and the deterministic/diffusion models that operate on the reduce-order space. A qualitative comparison is shown at Figure 5. We can see that all models’ predictions deviate from the reference numerical simulation after 5-th frame. For the latent space models, their predictions tend to be more physically coherent in the long run. We further look at the spectrum of different models’ prediction (Figure 2, 3, 4). All the models’ predictions match reference spectrum in low-frequency regime at the beginning, and FNO is better at the high-frequency regime due to the mesh-reduced nature of the latent space models. As time evolves, the error in the higher frequency regime of FNO’s prediction gradually transport to the low frequency regime, resulting in a distribution shift. For the latent space model, the error

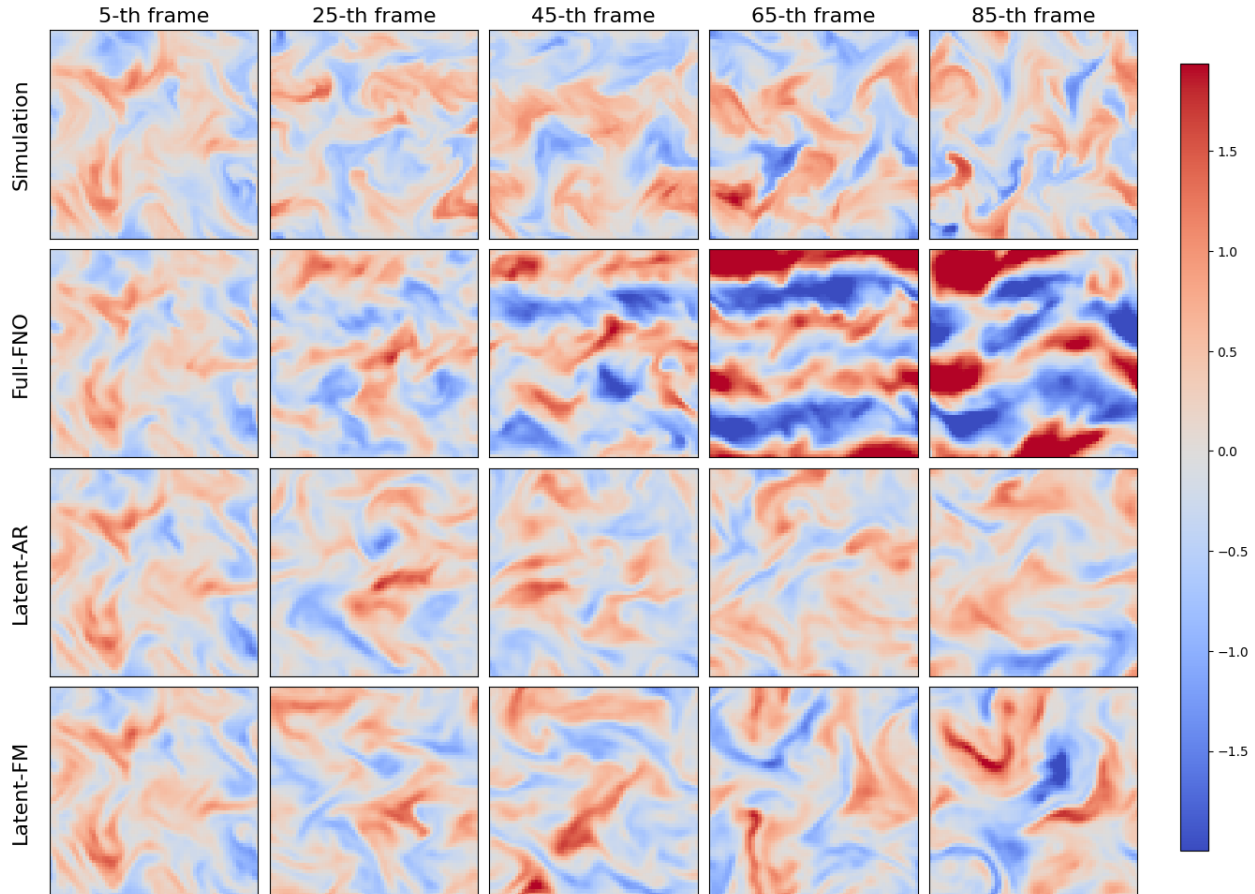


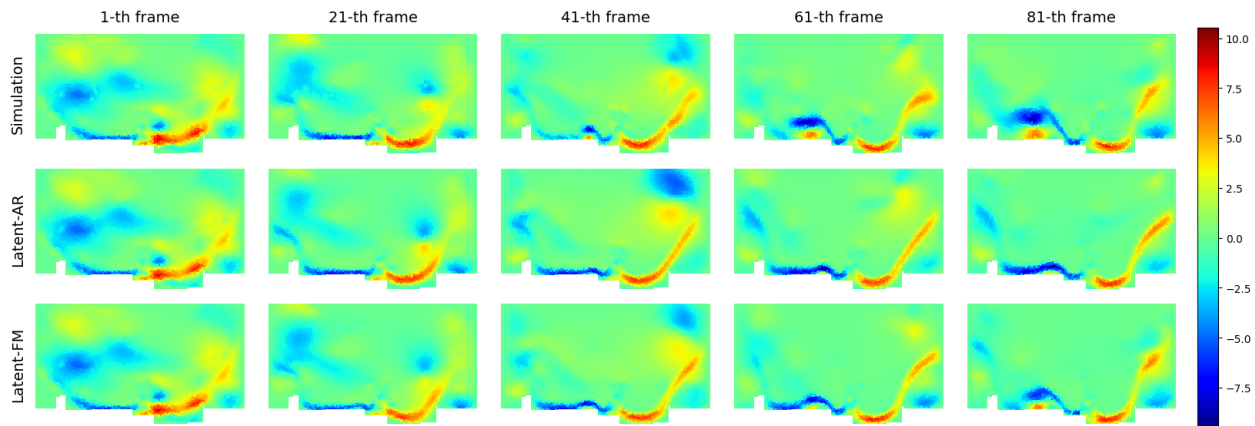
Figure 5: Visualization of the velocity field (x component) in 3D MHD predicted by different models.

accumulation in the spectrum is less pronounced and it can be observed that after a long rollout, the flow matching model generates more coherent spectrum.

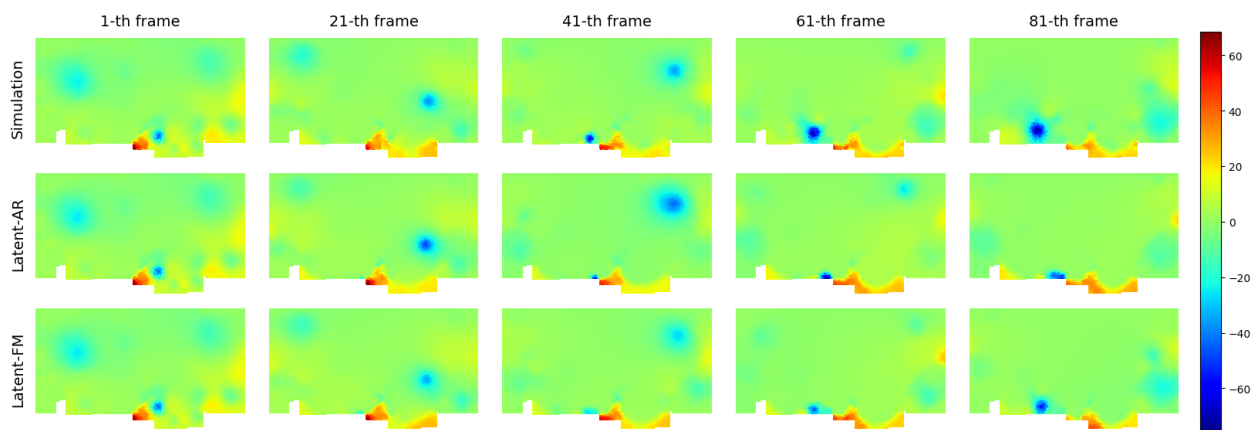
Time horizon	+1		+50		+250	
Variables	u	p	u	p	u	p
MeshGraphNet [30]	0.0810	0.4256	0.5926	2.2492	1.0702	3.7220
EAGLE Transformer [92]	0.0537	0.4590	0.3494	1.4432	0.6826	2.4130
Latent-AR	0.0766	0.0756	0.4216	0.4157	0.6678	0.5926
Latent-FM (ens=1)	0.0724	0.0720	0.4030	0.4115	0.6625	0.6077
Latent-FM (ens=8)	0.0765	0.0755	0.3925	0.3929	0.6360	0.5795

Table 4: NRMSE for different model’s prediction on EAGLE dataset. MeshGraphNet and EAGLE Transformer are trained with backprop-through-time on eight consecutive time steps.

The third problem is the 2D airflow around the UAV, which comprises a variety of different geometries and features fluid flow coupled with a moving UAV. Previous methods build graph neural networks (GNN) based on the simulation meshes, i.e. a graph with connectivity the same as the discretization mesh. In contrast, our proposed model is built on a unified latent grid. The quantitative comparison between different models are shown in Table 4. Overall, GNN-based models achieve slightly better accuracy in velocity prediction whereas the proposed latent flow matching model has significantly better accuracy in pressure prediction. We also find that the ensemble prediction notably improves the RMSE of model’s prediction in this problem. As shown in the qualitative comparison between deterministic latent models and stochastic ones, we observe that the proposed latent flow matching models can generate predictions that are more physically coherent with the reference numerical simulation.



(a) Visualization of different models' prediction on the x component of velocity field.



(b) Visualization of different models' prediction on the x component of pressure field.

Figure 6: Rollout visualization on EAGLE dataset.

5 Conclusion

In this work, we introduce a neural PDE solver that pairs diffusion-based training/sampling with a dimension-reduction autoencoder, projecting inputs from diverse meshes onto a lower-resolution latent grid. We analyze existing diffusion paths and proposed a modified flow-matching schedule that empirically outperforms other noise schedules. By leveraging multi-step diffusion—reminiscent of classical multi-step methods, our approach mitigates spectral artifacts and reduces compounding errors in chaotic, time-dependent systems. This framework not only enhances temporal stability but also lowers computational cost, offering robust, flexible modeling across various discretization grids. Overall, our generative latent PDE solver presents a scalable and adaptable alternative for designing temporal neural surrogate models.

References

1. Brandstetter, J., Worrall, D. & Welling, M. *Message Passing Neural PDE Solvers* 2023. arXiv: [2202.03376](https://arxiv.org/abs/2202.03376) [cs.LG]. <https://arxiv.org/abs/2202.03376>.
2. Li, Z. *et al. Learning Chaotic Dynamics in Dissipative Systems in Advances in Neural Information Processing Systems* (eds Koyejo, S. *et al.*) **35** (Curran Associates, Inc., 2022), 16768–16781. https://proceedings.neurips.cc/paper_files/paper/2022/file/6ad68277e27b42c60ac228c9859fc1a2-Paper-Conference.pdf.

3. Lippe, P., Veeling, B., Perdikaris, P., Turner, R. & Brandstetter, J. Pde-refiner: Achieving accurate long rollouts with neural pde solvers. *Advances in Neural Information Processing Systems* **36**, 67398–67433 (2023).
4. List, B., Chen, L.-W., Bali, K. & Thuerey, N. *Differentiability in Unrolled Training of Neural Physics Simulators on Transient Dynamics* 2024. arXiv: [2402.12971](https://arxiv.org/abs/2402.12971) [physics.comp-ph]. <https://arxiv.org/abs/2402.12971>.
5. Rahaman, N. *et al.* *On the Spectral Bias of Neural Networks* 2019. arXiv: [1806.08734](https://arxiv.org/abs/1806.08734) [stat.ML]. <https://arxiv.org/abs/1806.08734>.
6. Sanchez-Gonzalez, A. *et al.* *Learning to Simulate Complex Physics with Graph Networks* 2020. arXiv: [2002.09405](https://arxiv.org/abs/2002.09405) [cs.LG]. <https://arxiv.org/abs/2002.09405>.
7. Stachenfeld, K. *et al.* *Learned Simulators for Turbulence in International Conference on Learning Representations* (2022). <https://openreview.net/forum?id=msRBojTz-Nh>.
8. Werbos, P. Backpropagation through time: what it does and how to do it. *Proceedings of the IEEE* **78**, 1550–1560 (1990).
9. Lam, R. *et al.* *GraphCast: Learning skillful medium-range global weather forecasting* 2023. arXiv: [2212.12794](https://arxiv.org/abs/2212.12794) [cs.LG]. <https://arxiv.org/abs/2212.12794>.
10. Sohl-Dickstein, J., Weiss, E., Maheswaranathan, N. & Ganguli, S. *Deep Unsupervised Learning using Nonequilibrium Thermodynamics in Proceedings of the 32nd International Conference on Machine Learning* (eds Bach, F. & Blei, D.) **37** (PMLR, Lille, France, July 2015), 2256–2265. <https://proceedings.mlr.press/v37/sohl-dickstein15.html>.
11. Ho, J., Jain, A. & Abbeel, P. Denoising diffusion probabilistic models. *Advances in Neural Information Processing Systems* **33**, 6840–6851 (2020).
12. Song, Y. *et al.* *Score-Based Generative Modeling through Stochastic Differential Equations in International Conference on Learning Representations* (2021). <https://openreview.net/forum?id=PXTIG12RRHS>.
13. Zhou, A., Li, Z., Schneier, M., Jr, J. R. B. & Farimani, A. B. *Text2PDE: Latent Diffusion Models for Accessible Physics Simulation* 2025. arXiv: [2410.01153](https://arxiv.org/abs/2410.01153) [cs.LG]. <https://arxiv.org/abs/2410.01153>.
14. Shu, D., Li, Z. & Farimani, A. B. A physics-informed diffusion model for high-fidelity flow field reconstruction. *Journal of Computational Physics* **478**, 111972 (2023).
15. Kohl, G., Chen, L.-W. & Thuerey, N. *Benchmarking Autoregressive Conditional Diffusion Models for Turbulent Flow Simulation* 2024. arXiv: [2309.01745](https://arxiv.org/abs/2309.01745) [cs.LG]. <https://arxiv.org/abs/2309.01745>.
16. Huang, J., Yang, G., Wang, Z. & Park, J. J. *DiffusionPDE: Generative PDE-Solving Under Partial Observation* 2024. arXiv: [2406.17763](https://arxiv.org/abs/2406.17763) [cs.LG]. <https://arxiv.org/abs/2406.17763>.
17. Valencia, M. L., Pfaff, T. & Thuerey, N. *Learning Distributions of Complex Fluid Simulations with Diffusion Graph Networks in The Thirteenth International Conference on Learning Representations* (2025). <https://openreview.net/forum?id=uKZdlihDDn>.
18. Price, I. *et al.* *GenCast: Diffusion-based ensemble forecasting for medium-range weather* 2024. arXiv: [2312.15796](https://arxiv.org/abs/2312.15796) [cs.LG]. <https://arxiv.org/abs/2312.15796>.
19. Du, P., Parikh, M. H., Fan, X., Liu, X.-Y. & Wang, J.-X. *CoNFILD: Conditional Neural Field Latent Diffusion Model Generating Spatiotemporal Turbulence* 2024. arXiv: [2403.05940](https://arxiv.org/abs/2403.05940) [physics.flu-dyn]. <https://arxiv.org/abs/2403.05940>.
20. Lienen, M., Lüdke, D., Hansen-Palmus, J. & Günemann, S. *From Zero to Turbulence: Generative Modeling for 3D Flow Simulation* 2024. arXiv: [2306.01776](https://arxiv.org/abs/2306.01776) [physics.flu-dyn]. <https://arxiv.org/abs/2306.01776>.
21. Hang, T. *et al.* *Efficient Diffusion Training via Min-SNR Weighting Strategy* 2024. arXiv: [2303.09556](https://arxiv.org/abs/2303.09556) [cs.CV]. <https://arxiv.org/abs/2303.09556>.
22. Vincent, P. A Connection Between Score Matching and Denoising Autoencoders. *Neural Computation* **23**, 1661–1674 (2011).

23. Lipman, Y., Chen, R. T. Q., Ben-Hamu, H., Nickel, M. & Le, M. *Flow Matching for Generative Modeling in The Eleventh International Conference on Learning Representations* (2023). <https://openreview.net/forum?id=PqvMRDCJT9t>.
24. Liu, X., Gong, C. & qiang liu. *Flow Straight and Fast: Learning to Generate and Transfer Data with Rectified Flow in The Eleventh International Conference on Learning Representations* (2023). <https://openreview.net/forum?id=XVjTT1nw5z>.
25. Azizzadenesheli, K. *et al.* Neural operators for accelerating scientific simulations and design. *Nature Reviews Physics* **6**, 320–328 (2024).
26. Hao, Z. *et al.* Physics-informed machine learning: A survey on problems, methods and applications. *arXiv preprint arXiv:2211.08064* (2022).
27. Karniadakis, G. E. *et al.* Physics-informed machine learning. *Nature Reviews Physics* **3**, 422–440 (2021).
28. Guo, X., Li, W. & Iorio, F. *Convolutional Neural Networks for Steady Flow Approximation in Proceedings of the 22nd ACM SIGKDD International Conference on Knowledge Discovery and Data Mining* (Association for Computing Machinery, San Francisco, California, USA, 2016), 481–490. ISBN: 9781450342322. <https://doi.org/10.1145/2939672.2939738>.
29. Tompson, J., Schlachter, K., Sprechmann, P. & Perlin, K. *Accelerating Eulerian Fluid Simulation With Convolutional Networks in Proceedings of the 34th International Conference on Machine Learning* (eds Precup, D. & Teh, Y. W.) **70** (PMLR, June 2017), 3424–3433. <https://proceedings.mlr.press/v70/tompson17a.html>.
30. Pfaff, T., Fortunato, M., Sanchez-Gonzalez, A. & Battaglia, P. W. *Learning Mesh-Based Simulation with Graph Networks* 2021. arXiv: [2010.03409](https://arxiv.org/abs/2010.03409) [cs.LG]. <https://arxiv.org/abs/2010.03409>.
31. Li, Z., Meidani, K., Yadav, P. & Barati Farimani, A. Graph neural networks accelerated molecular dynamics. *The Journal of Chemical Physics* **156** (2022).
32. Li, Z. & Farimani, A. B. Graph neural network-accelerated Lagrangian fluid simulation. *Computers & Graphics* **103**, 201–211 (2022).
33. Lino, M., Fotiadis, S., Bharath, A. A. & Cantwell, C. D. Multi-scale rotation-equivariant graph neural networks for unsteady Eulerian fluid dynamics. *Physics of Fluids* **34**, 087110. ISSN: 1070-6631. eprint: https://pubs.aip.org/aip/pof/article-pdf/doi/10.1063/5.0097679/19818588/087110_1_online.pdf. <https://doi.org/10.1063/5.0097679> (Aug. 2022).
34. Lu, L., Jin, P., Pang, G., Zhang, Z. & Karniadakis, G. E. Learning nonlinear operators via DeepONet based on the universal approximation theorem of operators. *Nature Machine Intelligence* **3**, 218–229. ISSN: 2522-5839. <http://dx.doi.org/10.1038/s42256-021-00302-5> (Mar. 2021).
35. Kovachki, N. *et al.* Neural operator: Learning maps between function spaces with applications to pdes. *Journal of Machine Learning Research* **24**, 1–97 (2023).
36. Li, Z. *et al.* *Fourier Neural Operator for Parametric Partial Differential Equations in International Conference on Learning Representations* (2021). <https://openreview.net/forum?id=c8P9NQVtmm0>.
37. Gupta, G., Xiao, X. & Bogdan, P. *Multiwavelet-based Operator Learning for Differential Equations* 2021. arXiv: [2109.13459](https://arxiv.org/abs/2109.13459) [cs.LG]. <https://arxiv.org/abs/2109.13459>.
38. Fanaskov, V. & Oseledets, I. *Spectral Neural Operators* 2024. arXiv: [2205.10573](https://arxiv.org/abs/2205.10573) [math.NA]. <https://arxiv.org/abs/2205.10573>.
39. Li, Z. *et al.* *Geometry-Informed Neural Operator for Large-Scale 3D PDEs* 2023. arXiv: [2309.00583](https://arxiv.org/abs/2309.00583) [cs.LG]. <https://arxiv.org/abs/2309.00583>.
40. Li, Z. *et al.* *Multipole Graph Neural Operator for Parametric Partial Differential Equations* 2020. arXiv: [2006.09535](https://arxiv.org/abs/2006.09535) [cs.LG]. <https://arxiv.org/abs/2006.09535>.
41. Hao, Z. *et al.* *Gnot: A general neural operator transformer for operator learning in International Conference on Machine Learning* (2023), 12556–12569.
42. Wu, H., Luo, H., Wang, H., Wang, J. & Long, M. *Transolver: A Fast Transformer Solver for PDEs on General Geometries* 2024. arXiv: [2402.02366](https://arxiv.org/abs/2402.02366) [cs.LG]. <https://arxiv.org/abs/2402.02366>.

43. Li, Z., Shu, D. & Barati Farimani, A. Scalable transformer for pde surrogate modeling. *Advances in Neural Information Processing Systems* **36** (2024).
44. Li, Z., Meidani, K. & Farimani, A. B. Transformer for Partial Differential Equations’ Operator Learning. *Transactions on Machine Learning Research*. ISSN: 2835-8856. <https://openreview.net/forum?id=EPPqt3uERT> (2023).
45. Cao, S. Choose a transformer: Fourier or galerkin. *Advances in neural information processing systems* **34**, 24924–24940 (2021).
46. Raissi, M., Perdikaris, P. & Karniadakis, G. Physics-informed neural networks: A deep learning framework for solving forward and inverse problems involving nonlinear partial differential equations. *Journal of Computational Physics* **378**, 686–707 (2019).
47. Li, Z. *et al.* *Physics-Informed Neural Operator for Learning Partial Differential Equations* 2023. arXiv: [2111.03794 \[cs.LG\]](https://arxiv.org/abs/2111.03794). <https://arxiv.org/abs/2111.03794>.
48. Wang, S., Wang, H. & Perdikaris, P. Learning the solution operator of parametric partial differential equations with physics-informed DeepONets. *Science advances* **7**, eabi8605 (2021).
49. Benner, P., Gugercin, S. & Willcox, K. A survey of projection-based model reduction methods for parametric dynamical systems. *SIAM review* **57**, 483–531 (2015).
50. Berkooz, G., Holmes, P. & Lumley, J. L. The proper orthogonal decomposition in the analysis of turbulent flows. *Annual review of fluid mechanics* **25**, 539–575 (1993).
51. Lui, H. F. S. & Wolf, W. R. Construction of reduced-order models for fluid flows using deep feedforward neural networks. *Journal of Fluid Mechanics* **872**, 963–994 (2019).
52. Murata, T., Fukami, K. & Fukagata, K. Nonlinear mode decomposition with convolutional neural networks for fluid dynamics. *Journal of Fluid Mechanics* **882**, A13 (2020).
53. Maulik, R., Lusch, B. & Balaprakash, P. Reduced-order modeling of advection-dominated systems with recurrent neural networks and convolutional autoencoders. *Physics of Fluids* **33** (2021).
54. Fresca, S. & Manzoni, A. POD-DL-ROM: Enhancing deep learning-based reduced order models for nonlinear parametrized PDEs by proper orthogonal decomposition. *Computer Methods in Applied Mechanics and Engineering* **388**, 114181. ISSN: 0045-7825. <https://www.sciencedirect.com/science/article/pii/S0045782521005120> (2022).
55. Pan, S., Brunton, S. L. & Kutz, J. N. Neural implicit flow: a mesh-agnostic dimensionality reduction paradigm of spatio-temporal data. *Journal of Machine Learning Research* **24**, 1–60 (2023).
56. Chen, P. Y. *et al.* CROM: Continuous reduced-order modeling of PDEs using implicit neural representations. *arXiv preprint arXiv:2206.02607* (2022).
57. Serrano, L. *et al.* Operator learning with neural fields: Tackling pdes on general geometries. *Advances in Neural Information Processing Systems* **36**, 70581–70611 (2023).
58. Brunton, S. L., Budišić, M., Kaiser, E. & Kutz, J. N. *Modern Koopman Theory for Dynamical Systems* 2021. arXiv: [2102.12086 \[math.DS\]](https://arxiv.org/abs/2102.12086). <https://arxiv.org/abs/2102.12086>.
59. Lusch, B., Kutz, J. N. & Brunton, S. L. Deep learning for universal linear embeddings of nonlinear dynamics. *Nature Communications* **9**, 4950. ISSN: 2041-1723. <https://doi.org/10.1038/s41467-018-07210-0> (Nov. 2018).
60. Yin, Y., Kirchmeyer, M., Franceschi, J.-Y., Rakotomamonjy, A. & patrick gallinari. Continuous PDE Dynamics Forecasting with Implicit Neural Representations. <https://openreview.net/forum?id=B73niNjbPs> (2023).
61. Rojas, C. J., Dengel, A. & Ribeiro, M. D. Reduced-order model for fluid flows via neural ordinary differential equations. *arXiv preprint arXiv:2102.02248* (2021).
62. Hemmasian, A. & Barati Farimani, A. Reduced-order modeling of fluid flows with transformers. *Physics of Fluids* **35** (2023).
63. Vlachas, P. R., Arampatzis, G., Uhler, C. & Koumoutsakos, P. Multiscale simulations of complex systems by learning their effective dynamics. *Nat Mach Intell.* <https://doi.org/10.1038/s42256-022-00464-w> (2022).

64. Wiewel, S., Becher, M. & Thuerey, N. *Latent-space Physics: Towards Learning the Temporal Evolution of Fluid Flow* 2019. arXiv: [1802.10123](https://arxiv.org/abs/1802.10123) [cs.LG]. <https://arxiv.org/abs/1802.10123>.
65. Kontolati, K., Goswami, S., Karniadakis, G. E. & Shields, M. D. Learning in latent spaces improves the predictive accuracy of deep neural operators. *arXiv preprint arXiv:2304.07599* (2023).
66. Han, X., Gao, H., Pfaff, T., Wang, J.-X. & Liu, L.-P. Predicting physics in mesh-reduced space with temporal attention. *arXiv preprint arXiv:2201.09113* (2022).
67. Li, Z. *et al.* Latent neural PDE solver: A reduced-order modeling framework for partial differential equations. *Journal of Computational Physics* **524**, 113705 (2025).
68. Worrall, D. E., Cranmer, M., Kutz, J. N. & Battaglia, P. *Spectral Shaping for Neural PDE Surrogates* 2025. <https://openreview.net/forum?id=mmDkgLtYNI>.
69. McCabe, M., Harrington, P., Subramanian, S. & Brown, J. Towards stability of autoregressive neural operators. *arXiv preprint arXiv:2306.10619* (2023).
70. Raonic, B. *et al.* *Convolutional Neural Operators for robust and accurate learning of PDEs in Thirty-seventh Conference on Neural Information Processing Systems* (2023). <https://openreview.net/forum?id=MtekhXRP4h>.
71. Cao, S., Brarda, F., Li, R. & Xi, Y. *Spectral-Refiner: Accurate Fine-Tuning of Spatiotemporal Fourier Neural Operator for Turbulent Flows in The Thirteenth International Conference on Learning Representations* (2025). <https://openreview.net/forum?id=MKP1g8wUOP>.
72. Rombach, R., Blattmann, A., Lorenz, D., Esser, P. & Ommer, B. *High-Resolution Image Synthesis with Latent Diffusion Models* 2022. arXiv: [2112.10752](https://arxiv.org/abs/2112.10752) [cs.CV]. <https://arxiv.org/abs/2112.10752>.
73. Chung, H., Kim, J., Mccann, M. T., Klasky, M. L. & Ye, J. C. *Diffusion Posterior Sampling for General Noisy Inverse Problems* 2024. arXiv: [2209.14687](https://arxiv.org/abs/2209.14687) [stat.ML]. <https://arxiv.org/abs/2209.14687>.
74. Shysheya, A. *et al.* On conditional diffusion models for PDE simulations. *Advances in Neural Information Processing Systems* **37**, 23246–23300 (2024).
75. Shu, D. & Farimani, A. B. *Zero-Shot Uncertainty Quantification using Diffusion Probabilistic Models* 2024. arXiv: [2408.04718](https://arxiv.org/abs/2408.04718) [cs.LG]. <https://arxiv.org/abs/2408.04718>.
76. Liu, Q. & Thuerey, N. Uncertainty-aware surrogate models for airfoil flow simulations with denoising diffusion probabilistic models. *AIAA Journal* **62**, 2912–2933 (2024).
77. Li, T., Biferale, L., Bonaccorso, F., Scarpolini, M. A. & Buzzicotti, M. Synthetic Lagrangian turbulence by generative diffusion models. *Nature Machine Intelligence* **6**, 393–403 (2024).
78. Song, Y. & Ermon, S. Generative modeling by estimating gradients of the data distribution. *Advances in neural information processing systems* **32** (2019).
79. Song, J., Meng, C. & Ermon, S. *Denoising Diffusion Implicit Models in International Conference on Learning Representations* (2021). <https://openreview.net/forum?id=St1giarCHLP>.
80. Lu, C. *et al.* Dpm-solver: A fast ode solver for diffusion probabilistic model sampling in around 10 steps. *Advances in Neural Information Processing Systems* **35**, 5775–5787 (2022).
81. Zhang, Q. & Chen, Y. *Fast Sampling of Diffusion Models with Exponential Integrator in The Eleventh International Conference on Learning Representations* (2023). <https://openreview.net/forum?id=Loek7hfb46P>.
82. Lin, S., Liu, B., Li, J. & Yang, X. *Common Diffusion Noise Schedules and Sample Steps are Flawed* 2024. arXiv: [2305.08891](https://arxiv.org/abs/2305.08891) [cs.CV]. <https://arxiv.org/abs/2305.08891>.
83. Gupta, J. K. & Brandstetter, J. *Towards Multi-spatiotemporal-scale Generalized PDE Modeling* 2022. arXiv: [2209.15616](https://arxiv.org/abs/2209.15616) [cs.LG]. <https://arxiv.org/abs/2209.15616>.
84. Kingma, D. P. & Welling, M. *Auto-Encoding Variational Bayes* 2022. arXiv: [1312.6114](https://arxiv.org/abs/1312.6114) [stat.ML]. <https://arxiv.org/abs/1312.6114>.
85. Xie, X., Mowlavi, S. & Benosman, M. *Smooth and Sparse Latent Dynamics in Operator Learning with Jerk Regularization* 2024. arXiv: [2402.15636](https://arxiv.org/abs/2402.15636) [cs.LG]. <https://arxiv.org/abs/2402.15636>.

86. Vaswani, A. *et al.* *Attention Is All You Need* 2023. arXiv: [1706.03762](https://arxiv.org/abs/1706.03762) [cs.CL]. <https://arxiv.org/abs/1706.03762>.
87. Sahoo, S. S. *et al.* *Simple and Effective Masked Diffusion Language Models* 2024. arXiv: [2406.07524](https://arxiv.org/abs/2406.07524) [cs.CL]. <https://arxiv.org/abs/2406.07524>.
88. Peebles, W. & Xie, S. *Scalable Diffusion Models with Transformers* 2023. arXiv: [2212.09748](https://arxiv.org/abs/2212.09748) [cs.CV]. <https://arxiv.org/abs/2212.09748>.
89. Holl, P. & Thuerey, N. Φ_{Flow} (*PhiFlow*): *Differentiable Simulations for PyTorch, TensorFlow and Jax* in *International Conference on Machine Learning* (2024).
90. Burkhart, B. *et al.* The catalogue for astrophysical turbulence simulations (cats). *The Astrophysical Journal* **905**, 14 (2020).
91. Ohana, R. *et al.* *The Well: a Large-Scale Collection of Diverse Physics Simulations for Machine Learning* 2025. arXiv: [2412.00568](https://arxiv.org/abs/2412.00568) [cs.LG]. <https://arxiv.org/abs/2412.00568>.
92. JANNY, S. *et al.* *EAGLE: Large-scale Learning of Turbulent Fluid Dynamics with Mesh Transformers* in *The Eleventh International Conference on Learning Representations* (2023). <https://openreview.net/forum?id=mfIX4QpsARJ>.
93. Ronneberger, O., Fischer, P. & Brox, T. *U-Net: Convolutional Networks for Biomedical Image Segmentation* 2015. arXiv: [1505.04597](https://arxiv.org/abs/1505.04597) [cs.CV]. <https://arxiv.org/abs/1505.04597>.
94. Kossaifi, J., Kovachki, N., Azizzadenesheli, K. & Anandkumar, A. *Multi-Grid Tensorized Fourier Neural Operator for High-Resolution PDEs* 2023. arXiv: [2310.00120](https://arxiv.org/abs/2310.00120) [cs.LG]. <https://arxiv.org/abs/2310.00120>.
95. Liu, Z. *et al.* *A ConvNet for the 2020s* 2022. arXiv: [2201.03545](https://arxiv.org/abs/2201.03545) [cs.CV]. <https://arxiv.org/abs/2201.03545>.